Selective Isolation of *Electron* or *Hole* in Photocatalysis: ZnO-TiO_2 and TiO_2-ZnO Core-Shell Structured Heterojunction Nanofibers *via* Electrospinning and Atomic Layer Deposition

Fatma Kayaci,[a,b] Sesha Vempati,*[a] Cagla Ozgit-Akgun,[a,b] Inci Donmez, [a,b] Necmi Biyikli,[a,b] and Tamer Uyar*[a,b]

[a] UNAM-National Nanotechnology Research Center, Bilkent University, Ankara, 06800, Turkey

[b] Institute of Materials Science & Nanotechnology, Bilkent University, Ankara, 06800, Turkey

Authors for correspondence: SV: svempati01@qub.ac.uk; TU: uyar@unam.bilkent.edu.tr

Supplementary Information

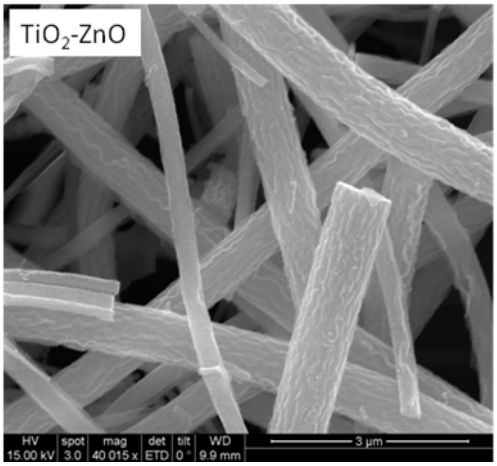

S1. Scanning electron microscope image of TiO_2-ZnO core-shell heterojunction nanofibers depicting the rough surface.

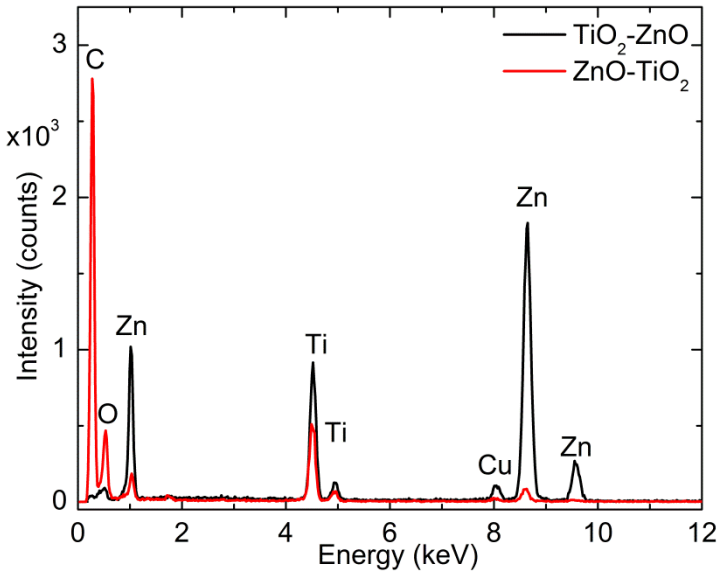

S2. EDX spectra of core-shell heterojunction ZnO-TiO_2 and TiO_2-ZnO nanofibers.

Anatase		Rutile		ZnO	
2θº	*hkl*	2θº	*hkl*	2θº	*hkl*
25.367	011	27.465	110	31.837	010
37.053	013	36.133	011	34.502	002
37.909	004	39.232	020	36.334	011
38.667	112	41.297	111	47.650	012
48.158	020	44.091	120	56.726	110
52.097	022	54.392	121	63.012	013
54.051	015	56.689	220	66.535	020
55.204	121	62.870	002	68.114	112
62.280	123	64.121	130	69.254	021
62.866	024	65.595	221	72.756	004
68.976	116	69.094	031	77.155	022
70.479	220	69.921	112	81.605	014
74.303	017	72.514	131	89.860	023
75.277	125	74.489	230		
76.247	031	76.667	022		
78.913	026	79.965	122		
81.028	008	82.448	231		
82.402	033	84.355	040		
82.927	224	87.592	140		
83.400	132	89.703	222		

S3. XRD peak list and the corresponding *hkl* indices for the two phases of TiO_2 (Anatase and Rutile) and ZnO.

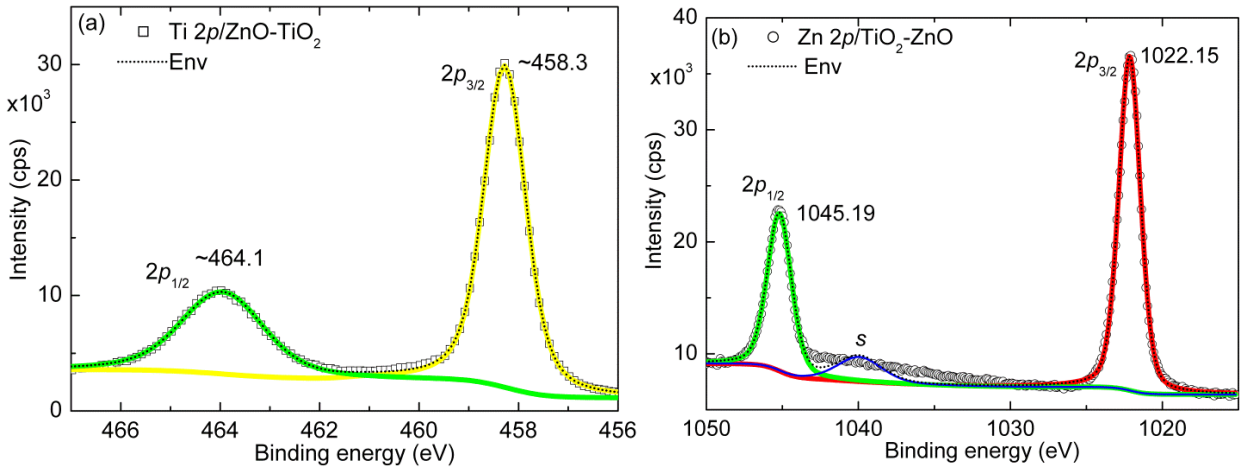

S4. Core-level XPS spectra of core-shell heterojunction nanofibers (a) Ti 2*p* region for ZnO-TiO_2 and (b) Zn 2*p* region for TiO_2-ZnO.

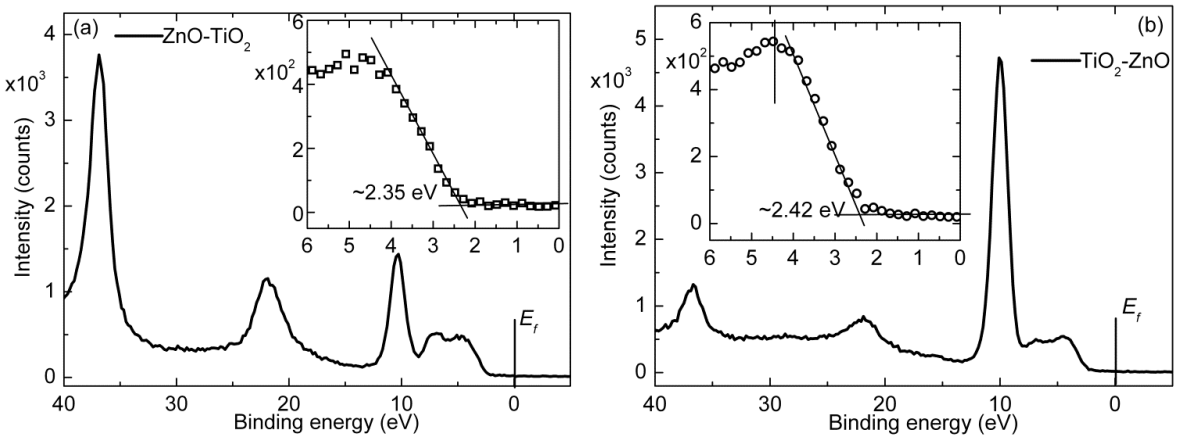

S5. Valance band XPS spectra of core-shell heterojunction nanofibers (a) ZnO-TiO_2 and (b) TiO_2-ZnO.

Process	***t***	***t* (ns)**	**Nature of the trap**
Generation			
$TiO_2 + h\nu \rightarrow e^-_{CB} + h^+_{VB}$	fs	~0.001	
Trapping			
$h^+_{VB} + >Ti^{IV}OH \rightarrow \{Ti^{IV}OH^{\bullet}\}$	10 ns	10	
$e^-_{CB} + >Ti^{IV}OH \leftrightarrow \{>Ti^{III}OH\}$	100 ps	0.1	Shallow traps; dynamic equilibrium
$e^-_{CB} + >Ti^{IV} \rightarrow >Ti^{III}$	10 ns	10	Deep trap; irreversible
Recombination			
$e^-_{CB} + \{>Ti^{IV}OH^{\bullet}\} \rightarrow >Ti^{IV}OH$	100 ns	100	
$h^+_{VB} + \{>Ti^{III}OH\} \rightarrow Ti^{IV}OH$	10 ns	10	
Transfer			
$\{Ti^{IV}OH^{\bullet}\}^+ + Red \rightarrow >Ti^{IV}OH + Red^{\bullet+}$	100 ns	100	
$e^-_{tr} + Ox \rightarrow >Ti^{IV}OH + Ox^{\bullet-}$	ms	~n10^6	

S6. Various fundamental processes on the surface of TiO_2 and their time scales [M. R. Hoffmann et al., Chem. Rev., 1995, Vol. 95, pp. 69-96] where *t*-characteristic time, e^-_{CB}-electron in conduction band (CB), h^+_{VB}-hole in valance band, >TiOH- primary hydrated (titanol) surface functionality of TiO_2 [W. Stumm, Chemistry of the Solid Water interface, Wiley-Interscience: New York, 1992; p 428], Red-reductant which is an electron donor, e^-_{tr} trapped electron, Ox-oxidant which is an electron acceptor, $\{>Ti^{IV}OH^{\bullet}\}^+$ surface trapped valance band hole (surface bound hydroxyl radical) and $\{>Ti^{III}OH\}$ surface trapped CB electron. Dynamic equilibrium: reversible trapping of an electron from CB in a shallow trap below the CB edge such that there is a certain possibility that e^-_{tr} - can be transferred back to the CB at RT.